

## Quantum statistical approach to Debye-Waller factor in EXAFS: application to monatomic fcc systems

Hiroaki Katsumata,<sup>a#</sup> Takafumi Miyanaga,<sup>b</sup> Toshihiko Yokoyama,<sup>a</sup> Takashi Fujikawa<sup>c</sup> and Toshiaki Ohta<sup>a</sup>

<sup>a</sup>Graduate School of Science, The University of Tokyo, 7-3-1 Hongo, Bunkyo-ku, Tokyo 113-0033 Japan.

<sup>b</sup>Faculty of Science and Technology, Hirosaki University, Bunkyo-cho 3, Hirosaki, Aomori 036-8561 Japan.

<sup>c</sup>Graduate School of Science, Chiba University, Yayoi-cho 1-33, Inage-ku, Chiba 263-8522 Japan.

E-mail: katumata@chem.s.u-tokyo.ac.jp

Temperature dependence of the Debye-Waller factors in EXAFS is studied for monatomic fcc lattice by use of the perturbation approach in terms of temperature Green's function. We apply the theory to the temperature dependence of EXAFS for Kr and Ni crystals. Furthermore we make a comparison among sc, bcc and fcc lattices for the present *ab initio* calculations.

**Keywords:** Debye-Waller-factors; monatomic fcc lattice; perturbation approach; temperature Green's function; EXAFS cumulant; Kr and Ni crystals.

### 1. Introduction

So far several theoretical approaches have been developed to describe the EXAFS cumulants including anharmonicity. Some of them are the perturbation approaches (Fujikawa and Miyanaga, 1993), while others are non-perturbation approaches by use of the path integral theory (Fujikawa et al., 1997; Yokoyama, 1998). In particular, perturbation approaches formulated by using temperature Green's functions provide wide applicability; we can apply the resummation technique with an aid of the diagrammatic technique. Here we focus our attention to weakly anharmonic systems, where typical low-order cumulant expansion works well.

In this work we apply the above perturbation approach to the analyses of the temperature dependence of EXAFS Debye-Waller factors. We focus our discussion on the new features in the temperature dependence of the Debye-Waller factors for three dimensional crystals compared with the previous works for low dimensional ones (Miyanaga and Fujikawa, 1994a, b).

### 2. Temperature Green's function formula of EXAFS Debye-Waller Factors

The theoretical approach used in this work is based on the temperature Green's function method developed by Fujikawa and Miyanaga (1993). The second, third and fourth order cumulants ( $M_2$ ,  $M_3$  and  $M_4$ ) are explicitly shown in that paper. We now apply this method to the monatomic fcc lattice with anharmonic Morse potentials between nearest neighbor atoms. It is assumed that the nearest neighbor interaction is described by the Morse potential as

$$V(x) = D(e^{-2\alpha x} - 2e^{-\alpha x}) \quad (1)$$

where  $x$  is the scaled relative deviation

$$x = (\ell - a)/a, \quad (2)$$

and  $\ell$  and  $a$  are the instantaneous and equilibrium distances between nearest neighbor atoms, respectively. The second order cumulant  $M_2$  is written as the sum of harmonic  $M_{20}$  and anharmonic  $M_{21}$  ( $M_2 = M_{20} + M_{21}$ ). In this calculation, phonon spectra  $\omega_j(\mathbf{k})$  and the associated eigenvectors  $e_j(\mathbf{k})$  are needed, which can be obtained by solving the dynamical matrix, and one million momenta  $\mathbf{k}$ 's in the first Brillouin zone are used.

### 3. Results and Discussion

First we study the shell dependence of the harmonic second and the third order cumulants. Figure 1 shows the temperature dependence of dimensionless harmonic second order cumulant  $\tilde{M}_{20} = M_{20}/(\hbar a/\pi a\sqrt{2DM})$ , where  $M$  is atomic mass and  $\tilde{T}_m$  is dimensionless temperature defined by  $\tilde{T}_m = k_B T/\hbar\omega_m$  ( $\omega_m = \sqrt{8D\alpha^2/Ma^2}$ ). In the previous work for one-dimensional monatomic crystal, the second order cumulant simply increases with the shell (Miyanaga and Fujikawa, 1994). In this case, that for the second shell is larger than for the nearest neighbor (first) shell, but those for the third and the fourth shells are as large as that for the second one. Figure 2 shows the temperature dependence of dimensionless third order cumulant  $\tilde{M}_3 = M_3/3a\hbar^2(4\alpha\pi^2MD)^{-1}$ . Although third order cumulant also increases with the shell for one-dimensional monatomic crystal, that for the first shell is the largest and that for the second shell is very small in the present case. The third order cumulant for the third shell is much larger than that for the second shell, but, is smaller than that for the fourth shell. Those results are consistent with the experimental results (Yokoyama et al., 1997; Yokoyama, 1998).

Secondly we compare the calculated and experimental cumulant for Kr and Ni crystals. For the Morse parameters for Ni crystal, those derived by Milstein (1973) are used. For Kr crystal, the employed pair potential is the one given by Barker et al. (1974), which is fitted with the Morse potential. The parameters used for the Kr and Ni crystals are as follows:

$$\begin{aligned} \text{Kr} \Rightarrow & D = 0.316 \times 10^{-20} \text{ J}, & \alpha = 6.133, \\ & a = 4.00787 \text{ \AA}, & M = 13.916 \times 10^{-26} \text{ kg}. \\ \text{Ni} \Rightarrow & D = 0.351 \times 10^{-19} \text{ J}, & \alpha = 6.288, \\ & a = 2.486 \text{ \AA}, & M = 9.746 \times 10^{-26} \text{ kg}. \end{aligned}$$

Figure 3 compares the calculated and experimental second order cumulant  $M_2$  for Kr crystal measured by Yokoyama et al. (1997). In this case,  $M_2$  for the first and the third shell are separately shown. A good agreement is obtained. Figures 4 and 5 compares the calculated and experimental third and fourth order cumulants,  $M_3$  and  $M_4$  for the Kr crystal. The results only for the first shell is shown. Again the present calculations well predict the experimental result without using additional fitting parameters. Figure 6 compares the calculated and experimental second order cumulant  $M_2$  for the Ni crystal measured by Yokoyama (1998). In this case,  $M_2$  for the first and the second shells are separately shown. Figure 7 compares the calculated and experimental third order cumulant  $M_3$  for the Ni crystal only for the first shell. We

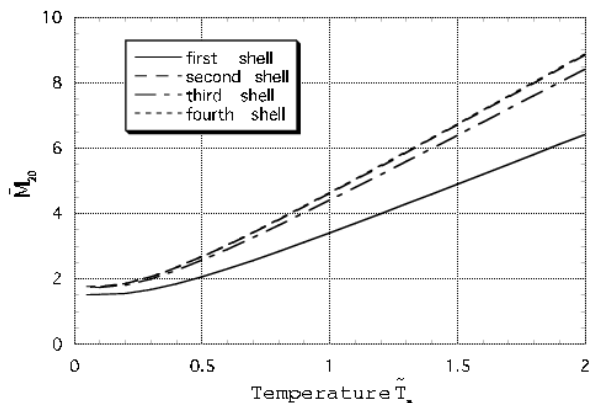


**Figure 1**  
Temperature dependence of the dimensionless harmonic second order cumulant  $\tilde{M}_{20}$  for the monatomic fcc lattice.

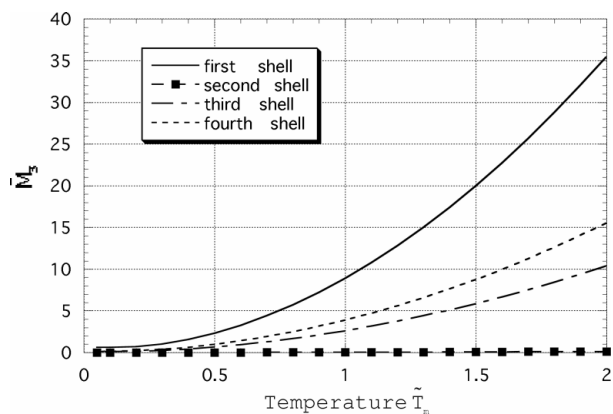


**Figure 2**  
Temperature dependence of the dimensionless third order cumulant  $\tilde{M}_3$  for the monatomic fcc lattice.

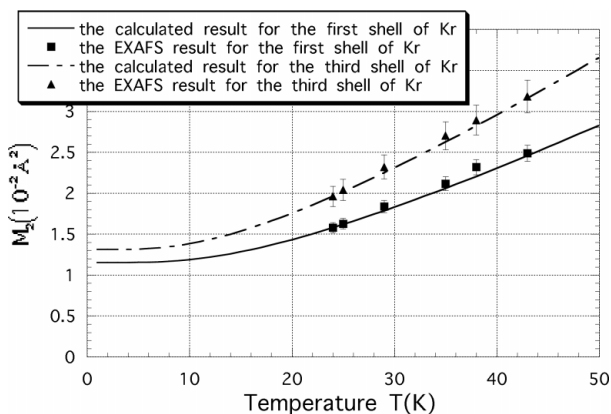


**Figure 3**  
Temperature dependence of the second order cumulant  $M_2$  for Kr.

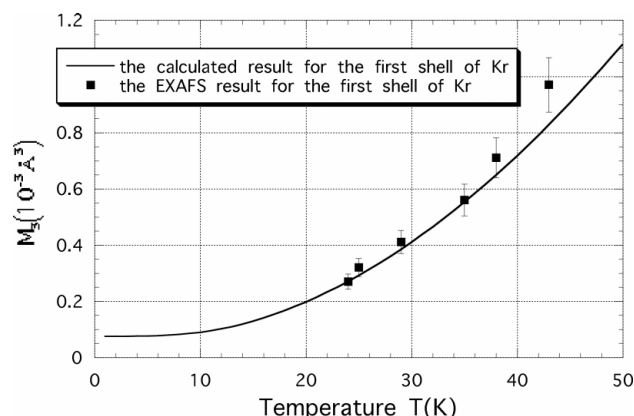


**Figure 4**  
Temperature dependence of the third order cumulant  $M_3$  for Kr.

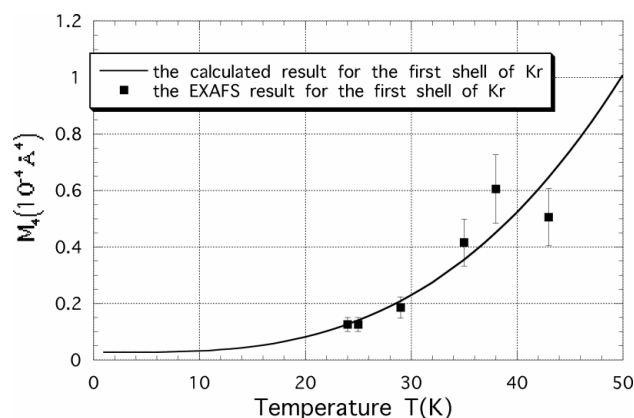


**Figure 5**  
Temperature dependence of the fourth order cumulant  $M_4$  for Kr.

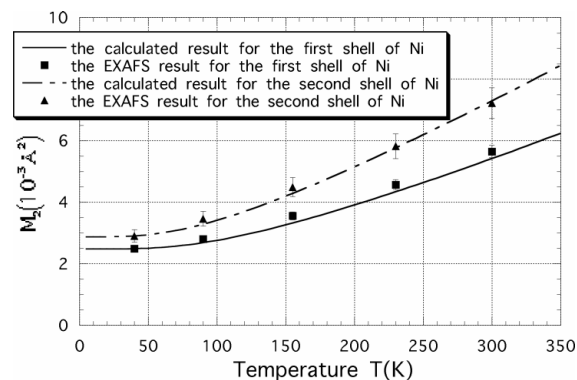


**Figure 6**  
Temperature dependence of the second order cumulant  $M_2$  for Ni.

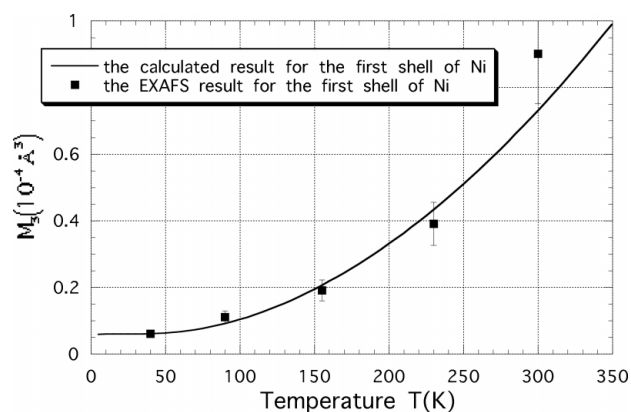


**Figure 7**  
Temperature dependence of the third order cumulant  $M_3$  for Ni.

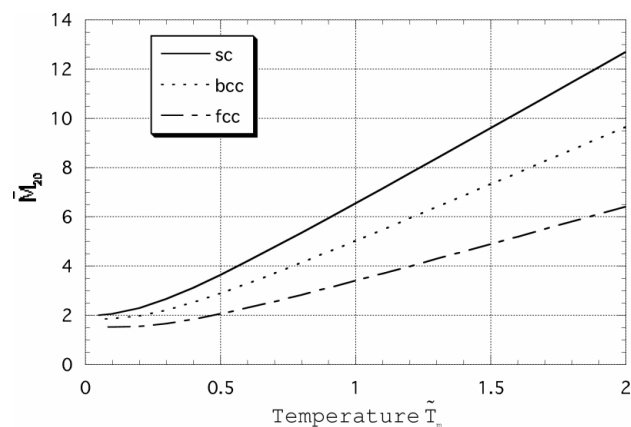


**Figure 8**  
Temperature dependence of the dimensionless harmonic 2nd order cumulant  $\tilde{M}_{20}$  for sc, bcc and fcc monatomic lattices for the first shell.  $\alpha = 6$  was assumed in all the calculations.

also find a good agreement between the calculated and the experimental results for the Ni crystal.

Lastly we make a comparison among sc, bcc and fcc lattices for the calculated results. Figure 8 shows the comparison of the dimensionless harmonic second order cumulant  $\tilde{M}_{20}$  for different crystal structures, sc, bcc and fcc lattices. We study the temperature dependence of  $\tilde{M}_{20}$  for the nearest neighbor atoms, where the equilibrium nearest neighbor distances are the same. We found that  $\tilde{M}_{20}$  becomes larger in turn of sc, bcc and fcc lattices (sc>bcc>fcc). This behavior is consistent with the expected trend due to the progressively increasing number of nearest neighbors going from the sc to fcc structures. For the dimensionless third order cumulant  $\tilde{M}_3$ , the similar result is obtained.

## 4. Conclusion

We obtain some characteristic features of the EXAFS cumulants for the three dimensional monatomic fcc system, which are quite different from those for one dimensional crystals. The present *ab initio* calculations based on the perturbation theory by Fujikawa and Miyanaga predict well the experimental results. Furthermore we can explain the difference in the EXAFS cumulant among sc, bcc and fcc lattices.

## References

- Barker, J. A., Watts, R. O., Lee, J. K., Schafer, T. P. and Lee, Y. T. (1974). *J. Chem. Phys.* **61**, 3081-3089.
- Fujikawa, T. & Miyanaga, T. (1993). *J. Phys. Soc. Jpn.* **62**, 4108-4122.
- Fujikawa, T., Miyanaga, T. & Suzuki, T. (1997). *J. Phys. Soc. Jpn.* **66**, 2897-2906.
- Milstein, F. (1973). *J. Appl. Phys.* **44**, 3825-3832.
- Miyanaga, T. & Fujikawa, T. (1994a). *J. Phys. Soc. Jpn.* **63**, 1036-1052.
- Miyanaga, T. & Fujikawa, T. (1994b). *J. Phys. Soc. Jpn.* **63**, 3683-3690.
- Yokoyama, T. (1998). *Phys. Rev.* **B57**, 3423-3432.
- Yokoyama, T., Ohta, T. & Sato, H. (1997). *Phys. Rev.* **B55**, 11320-11329.